

2
3
4 **A promising new baseflow method and recession**
5 **approach for streamflow at Glendhu Catchment, New**
6 **Zealand**

7
8
9
10 **M. K. Stewart¹**

11
12 ¹Aquifer Dynamics & GNS Science, PO Box 30368, Lower Hutt 5040, New Zealand

13
14 Correspondence to: M.K. Stewart (m.stewart@gns.cri.nz)

15
16

17 **Abstract**

18

19 Understanding and modelling the relationship between rainfall and runoff has been a
20 driving force in hydrology for many years. Baseflow separation and recession analysis
21 have been two of the main tools for understanding runoff generation in catchments, but
22 there are many different methods for each and no consensus on how best to apply them.
23 The new baseflow separation method presented here (the bump and rise method or BRM)
24 simulates the shape of tracer-determined baseflow or pre-event water more accurately
25 than previous methods. Application of the method by calibrating its parameters, using (a)
26 tracer data or (b) an optimizing method, is demonstrated for the Glendhu Catchment,
27 New Zealand. The calibrated algorithm is then applied to the Glendhu streamflow record.
28 The new recession approach advances the thesis that recession analysis of streamflow
29 alone gives misleading information on catchment storage reservoirs because streamflow
30 is a varying mixture of components of very different origins and characteristics (at the
31 simplest level, quickflow and baseflow as identified by the BRM method). Recession
32 analyses of quickflow, baseflow and streamflow show that the steep power-law slopes
33 often observed for streamflow at intermediate flows are artifacts due to such mixing and
34 are not representative of catchment reservoirs. Applying baseflow separation before
35 recession analysis could shed new light on water storage reservoirs in catchments and
36 possibly resolve some current problems with recession analysis. Among other things it
37 shows that both quickflow and baseflow reservoirs in the studied catchment have (non-
38 linear) quadratic characteristics.

39

40 1 Introduction

41

42 Interpretation of streamflow variations in terms of catchment characteristics has been a
43 major theme in hydrology for many years in order to improve catchment and stream
44 management. Two of the main tools for this task are baseflow separation and recession
45 analysis (Hall, 1968; Brutsaert and Nieber, 1977; Tallaksen, 1995; Smakhtin, 2001).
46 Baseflow separation aims to separate streamflow into two components (quickflow and
47 baseflow), where quickflow is direct runoff following rainfall, and baseflow is delayed
48 streamflow during periods without rain. Recession analysis aims to model the decrease of
49 streamflow during rainless periods to extract parameters descriptive of water storage in
50 the catchment. In a similar way, transit time analysis determines transit time distributions
51 of water in the stream and catchment in order to quantify flowpaths and storages through
52 the catchment. To fully understand and satisfactorily model the movement of water and
53 chemicals through catchments, it is necessary to understand in detail the water stores and
54 flowpaths (Fenicia et al., 2011; McMillan et al., 2011; Beven et al., 2012; Hrachowitz et
55 al., 2013).

56

57 The technique of baseflow separation has a long history in practical and scientific
58 hydrology because knowledge about baseflow is very useful in predicting low flow
59 progressions and understanding water quality variations. However, the many baseflow
60 separation methods have been regarded with suspicion for a long time because they were
61 often associated with “the Hortonian view of catchments” (Beven, 1991) or were
62 considered “to a large extent, arbitrary” (Hewlett and Hibbert, 1967). Nevertheless,
63 arbitrary as they may be, most of the methods yield results that are quite similar (e.g.
64 Gonzales et al., 2009 obtained long-term baseflow fractions (i.e. baseflow indexes, called
65 BFIs below) ranging from 0.76 to 0.91 for nine non-tracer baseflow separation methods,
66 not too different from their tracer-based result of 0.90), and all show that baseflow is
67 often quantitatively important in annual flows and, of course, very important during low
68 flows. This work contends that baseflow should also be considered during middle and
69 high flows, because streamflow during such events is composed of comparable amounts
70 of both quickflow and baseflow (e.g. Sklash and Farvolden, 1979) and they are produced
71 by very different mechanisms. It is believed that process descriptors such as hydrograph
72 recession constants (or transit time distribution parameters) should be determined on
73 separated components, not total streamflow, because the latter is a mixture and therefore
74 gives misleading results. All such process descriptors should be qualified by the
75 components they were derived from. Putting it simply, the contention is that to properly
76 understand the streamflow hydrograph it is first necessary to separate it into its quickflow
77 and baseflow components. While this may be considered obvious by some, recession
78 analysis has not previously been applied to other than the total streamflow.

79

80 Recession analysis also has a long history for practical hydrology reasons, but Stoelzle et
81 al. (2013) recently highlighted large discrepancies between different methods of analysis,
82 in particular contrasting recession parameters derived by the methods of Brutsaert and
83 Nieber (1977), Vogel and Kroll (1992), and Kirchner (2009). Stoelzle et al. suggested
84 that “a multiple methods approach to investigate streamflow recession characteristics
85 should be considered”. This indicates that the general technique itself is in some disarray,
86 and that there is little general consensus on how best to apply recession analysis to
87 streamflow.

88

89 This paper presents a new method of baseflow separation (called the bump and rise
90 method or BRM) which simulates the shape of tracer-determined baseflow or pre-event
91 water more accurately than previous methods. The two BRM parameters are calibrated by
92 (a) fitting to tracer data if it is available, or (b) using an optimizing process if it is not.
93 The calibrated BRM filter is then applied to the streamflow record. Two other baseflow
94 separation methods (those of Hewlett and Hibbert (1967) and Eckhardt (2005)) are
95 compared with the BRM. . The paper also takes a fresh look at the application of
96 recession analysis for characterising runoff generation processes in the light of surprising
97 effects of first separating the baseflow. Recession analysis of streamflow can give
98 misleading slopes on a recession plot particularly at intermediate flows because
99 streamflow is a varying mixture of components (at the simplest level, quickflow and
100 baseflow). When quickflow, baseflow and streamflow are all analysed, the effect of the
101 more rapidly receding quickflow on the streamflow can be seen. The same procedure
102 gives insight into the processes of streamflow generation at each exceedence percentage
103 when applied to flow duration curves (Section 2.4). The methods are illustrated using
104 streamflow data from the Glendhu Catchment in Otago, South Island, New Zealand.
105
106

107 **2 Methods**

109 **2.1 Baseflow Separation**

110
111 Justification for making baseflow separations rests on the dissimilarity of quickflow and
112 baseflow generation processes in catchments. Evidence of this is given by the different
113 recession slopes, and chemical and stable isotope compositions of early and late
114 recessions in hydrographs (examples are given for Glendhu, see below). In addition,
115 transit times of stream water show great differences between quickflow and baseflow.
116 While quickflow is young (as shown by the variations of conservative tracers and
117 radioactive decay of tritium), baseflow can be much older with substantial fractions of
118 water having mean transit times beyond the reach of conservative tracer variations (4
119 years) and averaging 10 years as shown by tritium measurements (Stewart et al., 2010,
120 2012; Michel et al., 2014). For these reasons, it is believed that it is not justifiable to treat
121 the streamflow as a single component, but that at least two components should be
122 considered by applying baseflow separation to the hydrograph before analysis.
123

124 Streamflow at any time (Q_t) is composed of the sum of quickflow (A_t) and baseflow (B_t)
125

$$126 \quad Q_t = A_t + B_t \quad (1)$$

127
128 where time steps are indicated by the sequences ... Q_{t-1} , Q_t , Q_{t+1} ... etc. The time
129 increment is one hour in the examples given below, but can be days in larger catchments
130 or any regular interval. Quickflow or direct runoff results from rainfall events and often
131 drops to zero between events, while baseflow is continuous as long as the stream flows.
132 As shown by the names, the important distinction between them is the time of release of
133 water particles to the stream (i.e. their transit times through the catchment). They are
134 supplied by fast and slow drainages within the catchment, direct precipitation and fast
135 storage reservoirs (soil stores) supply quickflow, and slow storage reservoirs
136 (groundwater aquifers) supply baseflow. This simple separation has proven to be
137 effective in many catchments, and is practical for the general case considered here.
138 However, particular catchments may have a variety of different possible streamflow

139 components that could be separated in principle. Fig. 1 gives a recession curve showing
140 the two flow components and the early and late parts of the curve. The late part of the
141 recession curve starts when baseflow dominates streamflow (i.e. quickflow becomes very
142 small).

143

144 Many methods have been developed for baseflow separation (see reviews by Hall, 1968;
145 Tallaksen, 1995; Gonzales et al., 2009). Baseflow separation methods can be grouped
146 into three categories: analytical, empirical and chemical/isotopic or tracer methods.

147 Analytical methods are based on fundamental theories of groundwater and surface water
148 flows. Examples are the analytical solution of the Boussinesq equation, the unit
149 hydrograph model and theories for reservoir yields from aquifers (Boussinesq, 1877; Su,
150 1995; Nejadhashemi et al., 2003).

151

152 Empirical methods based on the hydrograph are the most widely used (Zhang et al.,
153 2013), because of the availability of such data. The methods include 1) recession analysis
154 (Linsley et al., 1975), 2) graphical methods, filtering streamflow data by various methods
155 (e.g. finding minima within predefined intervals and connecting them) (e.g. Sloto and
156 Crouse, 1996), 3) low pass filtering of the hydrograph (Eckhardt, 2005; Zhang et al.,
157 2013), and 4) using groundwater levels to calculate baseflow contributions based on
158 previously determined relationships between groundwater levels and streamflows (Holko
159 et al., 2002).

160

161 One widely-used empirical method for small catchments was proposed by Hewlett and
162 Hibbert (1967) who argued that: “since an arbitrary separation must be made in any case,
163 why not base the classification on a single arbitrary decision, such as a fixed, universal
164 method for separating hydrographs on all small watersheds?” They separated the
165 hydrograph into “quickflow” and “delayed flow” components by arbitrarily projecting a
166 line of constant slope from the beginning of any stream rise until it intersected the falling
167 side of the hydrograph. The steady rise is described by the equations

168

$$169 \quad B_t = B_{t-1} + k \quad \text{for} \quad Q_t > B_{t-1} + k \quad (2)$$

$$170 \quad B_t = Q_t \quad \text{for} \quad Q_t \leq B_{t-1} + k \quad (3)$$

171

172 where k is the slope of the dividing line. The slope they chose was $0.05 \text{ ft}^3/\text{sec}/\text{mile}^2/\text{hour}$
173 ($0.000546 \text{ m}^3/\text{s}/\text{km}^2/\text{h}$ or $0.0472 \text{ mm}/\text{d}/\text{h}$). This universal slope gives a firm basis for
174 comparison of BFIs between catchments.

175

176 Tracer methods use dissolved chemicals and/or stable isotopes to separate the hydrograph
177 into component hydrographs based on mass balance of water and tracers. Waters from
178 different sources are assumed to have unique and constant (or varying in a well-
179 understood way) compositions (Pinder and Jones, 1969; Sklash and Farvolden, 1979;
180 McDonnell et al., 1991). These tracer methods allow objective separation of the
181 hydrograph, but it is important to consider just what water components are being
182 separated. For example, deuterium varies much more in rainfall than it does in soil or
183 groundwater, which has average deuterium concentrations from contributions from
184 several past events. When the deuterium content of a particular rainfall is very high or
185 very low, it becomes an effective indicator of the presence of “event” water in the stream,
186 compared with the “pre-event” water already in the catchment before rainfall began (as
187 shown in Fig. 2a adapted from Bonell et al., 1990). Baseflow separations (i.e.
188 identification of a groundwater component) have been more specifically shown by three-

189 component separations using chemicals and stable isotopes (Bazemore et al., 1994;
 190 Hangin et al., 2001; Joerin et al., 2002; Iwagami et al., 2010). An example of separation
 191 of direct precipitation, acid soil and groundwater components using silica and calcium is
 192 given in Fig. 2b redrawn from Iorgulescu et al. (2005).

193
 194 A remarkable and by now well-accepted characteristic of these separations is that the
 195 components including groundwater often respond to rainfall as rapidly as the stream
 196 itself. Chapman and Maxwell (1996) noted that “hydrograph separation using tracers
 197 typically shows a highly responsive old flow”. Likewise Wittenberg (1999) comments
 198 “tracers such as ^{18}O ... and salt ... [show] that even in flood periods outflow from the
 199 shallow groundwater is the major contributor to streamflow in many hydrological
 200 regimes”. And Klaus and McDonnell (2013) observe “most [tracer studies] showed a
 201 large preponderance of pre-event water in the storm hydrograph, even at peak flow”. This
 202 has been a general feature in tracer studies and includes all of the components tested
 203 whether quickflow or baseflow (e.g. Hooper and Shoemaker, 1986; Bonell et al., 1990;
 204 Buttle, 1994; Gonzales et al., 2009; Zhang et al., 2013). In the case of groundwater, the
 205 rapid response is believed to be partially due to rapid propagation of rainfall effects
 206 downwards (by pressure waves or celerity) causing rapid water table rise and
 207 displacement of stored water near the stream (e.g. Beven, 2012, page 349; McDonnell
 208 and Beven, 2014; Stewart et al., 2007, page 3354).

209
 210 Chapman and Maxwell (1996) and Chapman (1999) compared baseflow separations
 211 based on digital filters (like the low pass filters referred to above) with tracer separations
 212 in the literature and identified a preferred two-parameter algorithm given by
 213

$$214 \quad B_t = \frac{m}{1+c} B_{t-1} + \frac{c}{1+c} Q_t \quad (4)$$

215
 216 which approximately matched the tracer separations. m and C are parameters identified
 217 by fitting to the pre-event hydrograph identified by tracers. Eckhardt (2005)
 218 demonstrated that some previously published digital filters (Lyne and Hollick, 1979;
 219 Chapman and Maxwell, 1996; Chapman, 1999) could be represented by a more general
 220 digital filter equation by assuming a linear relationship between baseflow and baseflow
 221 storage (see equation 9 below). Eckhardt’s filter is
 222

$$223 \quad B_t = \frac{(1-BFI_{max})aB_{t-1} + (1-a)BFI_{max}Q_t}{1-aBFI_{max}} \quad (5)$$

224
 225 where parameter a is a recession constant relating adjacent baseflow steps during
 226 recessions, i.e.

$$227 \quad B_t = aB_{t-1} \quad (6)$$

228
 229
 230 and is determined by recession analysis. On the other hand, there was no objective way to
 231 determine parameter BFI_{max} (the maximum value of the baseflow index that can be
 232 modeled by the algorithm corresponding to low-pass filtering of a wave of infinite
 233 length). Eckhardt (2005) suggested that typical BFI_{max} values can be found for classes of
 234 catchments based on their hydrological and hydrogeological characteristics. Others have
 235 pointed out that these BFI_{max} values should be regarded as first approximations, and more
 236 refined values can be determined using tracers (Eckhardt, 2008; Gonzales et al., 2009;
 237 Zhang et al., 2013), by a backwards filtering operation (Collischonn and Fan, 2013) or by

238 the relationship of two characteristic values from flow duration curves (i.e. Q_{90}/Q_{50} ,
239 Smakhtin, 2001; Collischonn and Fan, 2013).

240

241 **2.1.1 The new baseflow separation method**

242

243 The new baseflow separation method put forward in this paper (hereafter called the bump
244 and rise method or BRM) has an algorithm chosen to simulate tracer separations simply
245 but as accurately as possible. Tracer separations show rapid baseflow responses to storm
246 events (the “bump”), which is followed in the method by a steady rise in the sense of
247 Hewlett and Hibbert (1967) (the “rise”). The steady rise is justified by increase in
248 catchment wetness conditions and gradual replenishment of groundwater aquifers during
249 rainy periods. The size of the bump (f) and the slope of the rise (k) are parameters of the
250 recursive digital filter that can be applied to the streamflow record. The separation
251 procedure is described by the equations:

252

$$253 \quad B_t = B_{t-1} + k + f(Q_t - Q_{t-1}) \quad \text{for} \quad Q_t > B_{t-1} + k \quad (7)$$

$$254 \quad B_t = Q_t \quad \text{for} \quad Q_t \leq B_{t-1} + k \quad (8)$$

255

256 where f is a constant fraction of the increase or decrease of streamflow during an event.
257 The values of f and k can be determined from tracer measurements, like the parameters of
258 other digital filters. If no tracer information is available, f and k can be determined by an
259 optimization process as described in an earlier version of this paper (Stewart, 2014a). An
260 unusual feature of the BRM method is that two types of baseflow response are included, a
261 short-term response via the bump and a longer-term response via the rise.

262

263 **2.2 Recession Analysis**

264

265 Recession analysis also has a long history. Stoelzle (2013) recently highlighted
266 discrepancies between methods of extracting recession parameters from empirical data by
267 contrasting results from three established methods (Brutsaert and Nieber, 1977, Vogel
268 and Kroll, 1992, and Kirchner, 2009). They questioned whether such parameters are
269 really able to characterise catchments to assist modelling and regionalisation, and
270 suggested that researchers should use more than one method because specific catchment
271 characteristics derived by the different recession analysis methods were so different.

272

273 The issue of whether storages can be represented by linear reservoirs or require to be
274 treated as non-linear reservoirs has been widely discussed in the hydrological literature
275 (in the case of recession analysis by Brutsaert and Nieber, 1977, Tallaksen, 1995, Lamb
276 and Beven, 1997 and Fenicia et al., 2006, among others). Lamb and Beven (1997)
277 identified three different storage behaviours in the three catchments they studied. Linear
278 reservoirs only require one parameter each and are more tractable mathematically. They
279 are widely used in rainfall-runoff models. Non-linearity can be approximately
280 accommodated by using two or more linear reservoirs in parallel, but more parameters
281 are required (three in the case of two reservoirs). Linear storage is expressed by the
282 formulation

283

$$284 \quad V = Q/\beta \quad (9)$$

285

286 where V is storage volume, and β is a constant (with dimensions of T^{-1}). The exponential
287 relationship follows for baseflow recessions

288

289

$$Q_t = Q_o \exp(-\beta t) \quad (10)$$

290

291 where Q_o is the streamflow at the beginning of the recession.

292

293 However, evidence for non-linearity is strong (Wittenberg, 1999) and the non-linear
294 formulation is often used

295

296

$$V = eQ^b \quad (11)$$

297

298 where e and b are constants. This gives the recession equation

299

300

$$Q_t = Q_o \left[1 + \frac{(1-b)Q_o^{(1-b)}}{eb} t \right]^{1/(b-1)} \quad (12)$$

301

302 The exponent b has been found to take various values between 0 and 1.1, with an average
303 close to 0.5 (Wittenberg, 1999). $b=1$ gives the linear storage model (equations 8 and 9).

304 For $b=0.5$, equation 11 reduces to the quadratic equation

305

306

$$Q_t = Q_o \left[1 + \frac{1}{ae} \cdot Q_o^{0.5} \cdot t \right]^{-2} \quad (13)$$

307

308 This quadratic equation is similar to the equation derived much earlier by Boussinesq
309 (1903) as an analytical solution for drainage of a homogeneous groundwater aquifer
310 limited by an impermeable horizontal layer at the level of the outlet to the stream

311

312

$$Q_t = Q_o (1 + \alpha t)^{-2} \quad (14)$$

313

314 where α is

315

316

$$\alpha = KB/PL^2 \quad (15)$$

317

318 Here K is the hydraulic conductivity, P the effective porosity, B the effective aquifer
319 thickness, and L the length of the flow path. Dewandel et al. (2003) have commented that
320 only this quadratic form is likely to give correct values for the aquifer properties because
321 it is an exact analytical solution to the diffusion equation, albeit with simplifying
322 assumptions, whereas other forms (e.g. exponential) are approximations.

323

324 In order to generalise recession analysis for a stream (i.e. to be able to analyse the
325 stream's recessions collectively rather than individually) Brutsaert and Nieber (1977)
326 presented a method based on the power-law storage-outflow model, which describes flow
327 from an unconfined aquifer into a stream. The negative gradient of the discharge (i.e. the
328 slope of the recession curve) is plotted against the discharge, thereby eliminating time as
329 a reference. This is called a recession plot below (following Kirchner, 2009). To keep the
330 timing right, the method pairs streamflow $Q = (Q_{t-1} + Q_t)/2$ with negative streamflow
331 recession rate $-dQ/dt = Q_t - Q_{t-1}$.

332

333 Change of storage in the catchment is given by the water balance equation:

334

335

$$\frac{dV}{dt} = R - E - Q \quad (16)$$

336

337 where R is rainfall and E is evapotranspiration. Assuming no recharge or extraction, we
338 have

339

$$340 \quad \frac{dV}{dt} = -Q \quad (17)$$

341

342 from whence equation 10 leads to

343

$$344 \quad -\frac{dQ}{dt} = \frac{1}{eb} Q^{2-b} = cQ^d \quad (18)$$

345

346 The exponent d allows for both linear (d=1) and non-linear (d≠1) storage outflow
347 relationships, with d=1.5 giving the frequently observed quadratic relationship (equation
348 12). Authors who have investigated the dependence of -dQ/dt on Q for late recessions
349 (low flows) have often found d averaging close to 1.5 (e.g. Brutsaert and Nieber, 1977;
350 Wittenberg, 1999; Dewandel, 2005; Stoelzle et al., 2013). Higher values of d were often
351 found especially at higher flows, e.g. Brutsaert and Nieber (1977) found values of d = 3
352 for the early parts of recessions.

353

354 Recent work has continued to explore the application and possible shortcomings of the
355 recession plot method. Rupp and Selker (2006) proposed scaling of the time increment to
356 the flow increment which can greatly reduce noise and artifacts in the low-flow part of
357 the plot. Biswal and Marani (2010) identified a link between recession curve properties
358 and river network morphology. They found slopes of individual recession events in
359 recession plots (d values) averaging around 2 and ranging from 1.1 to 5.5. In a small (1
360 km²) catchment, McMillan et al. (2011) showed that individual recessions plotted on the
361 recession plot “shifted horizontally with season”, which they attributed to changes in
362 contributing subsurface reservoirs as streamflow levels changed with season. This
363 explanation is analogous to the approach below in that two water components with
364 different storage characteristics are implied. The slopes of individual recessions in their
365 analysis were in excess of 2 with the low-flow tails being very much steeper. In medium
366 to large catchments (100 - 6,414 km²), Shaw and Riha (2012) found curves of individual
367 recessions “shifted upwards in summer relative to early spring and late fall curves”,
368 producing a data cloud when recessions from all seasons were combined. They speculate
369 that the movement with season (which was similar, but less extreme to that seen by
370 McMillan et al., 2011 above) was due to seasonal changes of catchment
371 evapotranspiration. They found that the slopes of individual recessions were often close
372 to 2 and had an extreme range of 1.3 to 5.3.

373

374 Problems in determining recession parameter values from streamflow data on recession
375 plots are due to 1) different recession extraction methods (e.g. different selection criteria
376 for data points), and 2) different parameter-fitting methods to the power-law storage-
377 outflow model (equation 17). There is generally a very broad scatter of points on the
378 plots, which makes parameter-fitting difficult. Clearly evapotranspiration is likely to play
379 a role in producing some of the scatter because evapotranspiration was neglected from
380 equation 16.

381

382 **2.2.1 The New Recession Analysis Approach**

383

384 However, it is believed that part of the scatter as well as the steep slopes of recession
385 curves often observed at intermediate flows in recession plots are due to recession
386 analysis being applied to streamflow rather than to its separated components. As shown
387 below, the changing proportions of quickflow and baseflow in streamflow during early
388 parts of recessions cause recession analyses of streamflow to give mixed messages, i.e.
389 misleading results not characteristic of storages in the catchment because the storage for
390 each component is very different. This has probably led to some previous recession
391 analysis studies giving misleading results in regard to catchment storage in cases where
392 early recession streamflow has been analysed.

393 **2.3 Flow Duration Curves**

394

395 Flow duration curves (FDCs) represent in one figure the flow characteristics of a stream
396 throughout its range of variation. They are cumulative frequency curves that show the
397 percentages of time during which specified discharges were equalled or exceeded in
398 given periods. They are useful for practical hydrology (Searcy, 1959), and have been
399 used as calibration targets for hydrologic models (Westerberg et al., 2011).

400

401 FDCs can also be determined for the separated stream components as shown below (Fig.
402 5d). Although FDCs for streamflow are not misleading and obviously useful in their own
403 right, FDCs of separated components can give insight into the processes of streamflow
404 generation at each exceedence percentage.

405

406

407 **3 Results of Application of New Approaches to Glendhu GH1**

408 **Catchment**

409

410 The BRM baseflow separation method is applied to Glendhu GH1 catchment to
411 investigate its applicability, demonstrate how it is applied and present what it reveals
412 about the catchment. The results are compared with those from two other widely-used
413 baseflow separation filters, the Hewlett and Hibbert (1965) method (called the H & H
414 method below) and the Eckhardt (2005) method (called the Eckhardt method). We need
415 to know the values of the parameters of these methods in order to apply them, the
416 parameters are k (the universal slope of the rise through the event) for the H & H method,
417 BFI_{max} (the maximum value of the baseflow index that can be modeled by the Eckhardt
418 algorithm) and a (recession constant) for the Eckhardt method, and f (bump fraction) and
419 k (slope of the rise) for the BRM method.

420

421 The parameter k for the H & H method has the universal (arbitrary) value of 0.0472 mmd^{-1}
422 h^{-1} , as explained above. Estimation of the Eckhardt parameters is not so simple (see
423 above) and has similarities to the estimation of the BRM parameters. There are two ways
424 of determining the Eckhardt and BRM parameters: (1) By adjusting the baseflow
425 parameters to give the best fits between the baseflows and the tracer-determined pre-
426 event or baseflow water. This is regarded as the only objective way, and is able to be used
427 in this paper because deuterium data is available for Glendhu (Bonell et al., 1990). But it
428 requires tracer data during events which is not generally available for catchments. (2)
429 Where there is no tracer data, the parameters can be estimated in several ways. In the
430 prescribed Eckhardt method, a is calculated from the late part of the recession by an
431 objective procedure. BFI_{max} is estimated to a first approximation based on the
432 hydrological and hydrogeological characteristics of the catchment (Eckhardt (2005), and
433 possibly more precisely by hydrograph methods suggested by Collischonn and Fan

434 (2013) (see below). For the BRM, the BFI can be estimated approximately from
435 catchment considerations (in analogy with the Eckhardt method) and possibly more
436 precisely by a flow duration curve method suggested by Collischonn and Fan (2013).
437 The BFI can then be used as a constraint while optimising the fit between the sum and the
438 streamflow (where the sum equals the baseflow plus a fast recession). This optimising
439 procedure was used in the earlier version of this paper (Stewart, 2014a). The optimising
440 procedure was also applied to the H & H and Eckhardt methods in the Author's Reply
441 (Stewart, 2014b).

442
443 Once baseflow separation has been achieved, recession analysis via the recession plot can
444 be applied to the separated quickflow and baseflow components (the new approach
445 suggested here), in addition to the streamflow (the traditional method). Whereas the
446 streamflow can show high power law slopes (d values of 2 or more), the components
447 generally have slopes around 1.5. However, note that the baseflow is a subdued reflection
448 of the streamflow because of its calculation procedure (equations 6 and 7) in the early
449 part of the recession. In the late part of the recession, the baseflow and the streamflow are
450 the same. Flow duration curve analysis can also be applied to the components as well as
451 to the streamflow in order to show the makeup of the streamflow at each exceedence
452 percentage.

453
454 In the following, the characteristics of the Glendhu Catchment are briefly described, then
455 the three baseflow separation methods are applied and compared, and then the effects of
456 applying recession analysis and FDC analysis to the separated components as well as to
457 the streamflow itself are examined. The methods are then applied to the master recession
458 curve

459

460 **3.1 Hydrogeology of Glendhu Catchment**

461

462 GH1 catchment (2.18 km²) is situated 50 km inland from Dunedin in the South Island of
463 New Zealand. It displays rolling-to-steep topography and elevation ranges from 460 to
464 650 m.a.s.l. (Fig. 3). Bedrock is moderately-to-strongly weathered schist, with the
465 weathered material filling in pre-existing gullies and depressions. Much of the bedrock-
466 colluvial surface is overlain by a loess mantle of variable thickness (0.5 to 3 m). Well-to-
467 poorly drained silt loams are found on the broad interfluvies and steep side slopes, and
468 poorly drained peaty soils in the valley bottoms.

469

470 Amphitheatre-like sub-catchments are common features in the headwaters and frequently
471 exhibit central wetlands that extend downstream as riparian bogs. Snow tussock
472 (*Chionochloa rigida*) is the dominant vegetation cover and headwater wetlands have a
473 mixed cover of sphagnum moss, tussock, and wire grass (*Empodisma minus*). The mean
474 annual temperature within GH1 at 625 m.a.s.l. elevation is 7.6C, and the mean annual
475 rainfall is 1350 mm/a. Annual runoff is measured at all weirs to an accuracy of $\pm 5\%$
476 (Pearce et al., 1984).

477

478 Pearce et al. (1984) showed that GH1 and GH2 (before the latter was forested), had very
479 similar runoff ratios. Long term precipitation and runoff at GH1 weir average 1350 mm/a
480 and 743 mm/a respectively (Fahey and Jackson, 1997). Actual evapotranspiration of 622
481 mm/a was measured for tussock grassland in the period April 1985 to March 1986 at a
482 nearby site in catchment GH1 (570 m a.s.l.) by Campbell and Murray (1990) using a
483 weighing lysimeter. The Priestley-Taylor estimate of PET was 643 mm/a for the period,

484 and 599 mm/a for 1996, so ET for GH1 is taken as 600 mm/a. The GH1 hydrological
 485 balance is: Precipitation (1350 mm/a) – ET (600 mm/a) = Runoff (743 mm/a), and loss
 486 around the weir is clearly negligible (Pearce et al. 1984). Comparison of runoff from
 487 GH1 and GH2 (after the latter had been forested for 7 years), showed that there was a
 488 decrease of 260 mm/a in GH2 runoff due to afforestation (Fahey and Jackson, 1997).
 489 Consequently, the GH2 balance is: Precipitation (1350 mm/a) – ET (860 mm/a) = Runoff
 490 (483 mm/a). The increase in ET for GH2 is attributed to increased interception (with
 491 evaporative loss) and transpiration.

492
 493 Bonell et al. (1990) carried out separation of event and pre-event waters using deuterium
 494 and chloride concentrations to investigate the runoff mechanisms operating in GH1 and
 495 GH2 at Glendhu (see example in Fig. 2a). The results showed that for quickflow volumes
 496 greater than 10 mm (over the catchment area), the early part of the storm hydrograph
 497 could be separated into two components, pre-event water from a shallow unconfined
 498 groundwater aquifer, and event water attributed to “saturated overland flow” (Bonell et
 499 al., 1990). The pre-event water responded more rapidly to rainfall than event water. The
 500 late part of the storm hydrograph consisted of pre-event water only. Hydrographs for
 501 smaller storms had pre-event water only, but this may be partly because measurement
 502 accuracy of the deuterium may not have been sufficient to detect event water in these
 503 smaller events.

505 3.2 Application of Baseflow Separation Methods

506 Fig. 2a showed the pre-event component determined using deuterium during the large
 507 storm on 23 February 1988 (Bonell et al., 1990). The pre-event component has a BFI of
 508 0.529 during the event (Table 1). Baseflows determined by the three baseflow separation
 509 methods are compared with the pre-event component in Figs. 4a-c. The goodness of fit of
 510 the baseflows to the pre-event water was determined using least squares,

$$511 \quad 512 \quad 513 \quad sd = (\sum(B_i - PE_i)^2 / N)^{0.5} \quad (19)$$

514 where PE_i is the pre-event water at each time step, and N the number of values. The H &
 515 H baseflow is totally inflexible with a pre-determined parameter and does not match the
 516 BFI or shape of the pre-event hydrograph at all well (its BFI is 0.255 and sd is 6.41
 517 mm/d, Table 1, Fig. 4a).

518
 519 The Eckhardt baseflow with prescribed parameters ($BFI_{max} = 0.8$ for a porous perennial
 520 stream, $a = 0.99817$ calculated from the baseflow recession) does not match the pre-event
 521 hydrograph well either ($BFI = 0.272$, $sd = 6.34$ mm/d, Fig. 4c). However, a better match
 522 of the BFI and a slightly better fit is found with the optimized version when both BFI_{max}
 523 and a are treated as adjustable parameters using the method of Zhang et al., 2013 (i.e.
 524 BFI_{max} was adjusted first to match the Eckhardt BFI to the pre-event BFI, then a was
 525 adjusted to improve the fit between the shapes of the baseflow and the pre-event
 526 hydrographs, then the steps were repeated, etc.). An extra constraint was to prevent the
 527 Eckhardt baseflow falling too far below the streamflow at very low flows. These give a
 528 BFI of 0.524, which is the same as that of the pre-event hydrograph (0.529, Table 1), and
 529 the baseflow has a similar shape to the pre-event water (Fig. 4c), but the peak is delayed
 530 in time giving only a small improvement in the fit ($sd = 5.40$ mm/d).

531
 532 The BRM baseflow gives a BFI of 0.526, the same as that of the pre-event hydrograph,
 533 and the fit between the two hydrographs is very close ($sd = 1.98$ mm/d, Fig. 4e). This

534 reflects the choice of the algorithm to mimic tracer baseflow separations (equations 7 and
535 8), which it does very well.

536

537 The three methods have been applied to hourly streamflow data for 1996. A sample of
538 each is shown for a two-week period in Figs. 4b, 4d and 4f. Only this short period is
539 shown because otherwise it is difficult to see the baseflow clearly. The parameters used
540 are listed in Table 2 along with the annual BFI values determined. The H & H baseflow
541 rises gradually through the stormflow peak, then follows the falling limb of the
542 streamflow after it intersects with it. The prescribed Eckhardt baseflow also rises
543 gradually through the peak then stays close to the recessing streamflow. The optimised
544 Eckhardt baseflow rises sharply then falls sharply when it intersects the falling limb of
545 the streamflow, and then gradually falls below the recessing streamflow curve. The BRM
546 baseflow mirrors the streamflow peak then follows the falling streamflow after it
547 intersects with it. It is also instructive to compare the BFI values derived by the various
548 methods. The H & H method gives a BFI of 0.679, the Eckhardt methods BFIs of 0.617
549 and 0.754 and the BRM method a BFI of 0.780 (almost the same as the Q_{90}/Q_{50} -derived
550 BFI of 0.779, see below).

551

552 Table 2 also shows estimates based on the characteristic flows from the flow duration
553 curve (Q_{90}/Q_{50}). Smakhtin (2001) observed that the ratio of the two characteristic flows
554 could be used to estimate BFI, and Collischonn and Fan (2013) derived equations
555 connecting Q_{90}/Q_{50} and BFI_{max} and BFI based on results from fifteen catchments of
556 varying sizes in Brazil. Their equations were

557

$$558 \quad BFI_{max} = 0.832 \frac{Q_{90}}{Q_{50}} + 0.216 \quad (20)$$

559

$$560 \quad BFI = 0.850 \frac{Q_{90}}{Q_{50}} + 0.163 \quad (21)$$

561

562 These have been used to determine BFI_{max} and BFI in Table 2 (marked as FDC BFI_{max}
563 and FDC BFI for clarity) for comparison with those derived using the three baseflow
564 separation methods. There is a close correspondence between the FDC BFI and the BRM
565 BFI, as noted, but the others are not particularly close. The backwards filter method of
566 Collischonn and Fan (2013) has also been applied to estimate the BFI_{max} values for the
567 prescribed and optimized Eckhardt parameters (Table 2). The resulting BFIs do not agree
568 particularly well with the BFIs obtained from the other methods.

569

570 The second way of determining the BRM parameters was described in the earlier version
571 of this paper (Stewart, 2014a). Streamflow data was available for a summer month
572 (February 1996) and a winter month (August 1996). These had different BFIs, but the
573 bump fractions (f) obtained by finding the best-fits of the sum (i.e. baseflow plus fast
574 recession) to the streamflow were similar at 0.16, while the slopes (k) were different. The
575 fast recession was assumed to have a quadratic form (i.e. $d = 1.5$, equation 14) when
576 fitting the sum to the streamflow, but the exponential ($d = 1$) and reciprocal ($d = 2$) forms
577 were also tested and found to give the same quadratic result for the quickflow (i.e. slope
578 of $d = 1.5$ on Fig. 5c) (Stewart 2014a). This optimizing process was also applied to the
579 Eckhardt method in Stewart (2014b).

580

581 **3.3 Application of New Approach to Recession and Flow Duration Curve** 582 **Analysis**

583

584 The recession behavior of the streamflow, BRM baseflow and BRM quickflow from the
585 hourly streamflow record during 1996 are examined on recession plots (i.e. $-dQ/dt$ versus
586 Q) in Figs. 5a-c. Discharge data less than two hours after rainfall has been excluded. The
587 three figures have the same two lines on each. The first is a line through the lower part of
588 the streamflow data with slope of 6 (this is called the streamflow line, see Fig. 5a). The
589 second is a line through the quickflow points with slope of about 1.5 (this is called the
590 quickflow line, see Fig. 5c). The streamflow points define a curve approaching the
591 quickflow line at high flows when baseflow makes up only a small proportion of the
592 streamflow, and diverging from it when baseflow becomes more important. The slope of
593 a line through the points becomes much steeper in this lower portion (as shown by the
594 streamflow line), The baseflow points (Fig. 5b) have a similar pattern to the streamflow
595 points because the BRM baseflow shape mimics the streamflow shape at high to medium
596 flows because of the form of equations 7 & 8. At low flows the baseflow plots on the
597 streamflow and hence shows the same low flow pattern as the streamflow.

598

599 Quickflow is determined by subtracting baseflow from streamflow (Equation 1). It rises
600 rapidly from zero or near-zero at the onset of rainfall to a peak two to three hours after
601 rainfall, then falls back to zero in around 24 to 48 hours unless there is further rain. The
602 quickflow points at flows above about 1 mm/d fall on the quickflow line with slope of
603 1.5. Errors become much larger as quickflow becomes very small (i.e. as baseflow
604 approaches streamflow and quickflow is the small difference between the two). As Rupp
605 and Selker (2006) have noted “time derivatives of Q amplify noise and inaccuracies in
606 discharge data”. Nevertheless the quickflow points show a clear pattern supporting near-
607 quadratic fast recessions. The streamflow points might be expected to show a recession
608 slope of 1.5 at very low flows as the streamflow becomes dominated by baseflow, but the
609 data may not be accurate enough to show this (see Section 3.4).

610

611 Flow duration curves for streamflow, baseflow and quickflow are given in Fig. 5d. The
612 streamflow FDC has a very shallow slope indicating groundwater dominance over the
613 higher exceedance percentages. Streamflow diverges noticeably from baseflow below
614 about 17% exceedance (when quickflow reaches about 10% of streamflow). This figure
615 reveals the reasons for breakpoints (i.e. changes of slope) in streamflow FDCs, which
616 have been related to contributions from different sources/reservoirs in catchments (Pfister
617 et al., 2014).

618

619

620 **3.4 “Master” recession curve for Glendhu**

621

622 Fig. 6a shows the master recession curve not involving snowmelt or additional rainfall,
623 derived by Pearce et al. (1984) from the longest recessions observed during a three year
624 study period in GH1 and GH2 (before afforestation of GH2). The data for the curve come
625 from four storm events during winter and six during summer. These authors reported that
626 “This recession curve is typical of high to medium runoff events. The plot shows that
627 there is a marked change of slope between the early and late parts of the recessions (at a
628 flow of about 2.6 mm/d). Quickflow, as defined by the method of Hewlett and Hibbert
629 (1967), comprises 30% of the annual hydrograph and ceases shortly after the change in
630 recession rate in most hydrographs.”

631

632 The streamflow points from the master curve have been fitted by the sum of a quadratic
633 fast recession curve and the baseflow (Fig. 6b). The baseflow was calculated using the
634 parameters identified by the fitting to the pre-event hydrograph above ($f = 0.40$, $k = 0.009$
635 $\text{mm d}^{-1} \text{h}^{-1}$, Table 2). These parameters give a BFI of 0.828. During the late part of the
636 recession, when the baseflow dominates the streamflow, a slow recession curve was fitted
637 to the streamflow. The data are given in Table 2. The sum fits all of the points well and
638 there is a smooth transition between the early and late parts of the recession. The
639 inflexion point (Fig. 7b) occurs when the baseflow stops falling and begins to rise. The
640 inflexion point is therefore an expression of the change from the bump to the rise in the
641 baseflow and supports the BRM baseflow separation method. The change from early to
642 late recession when baseflow begins to dominate the recession comes considerably after
643 the inflexion point (Fig. 6b).

644

645 It is also instructive to see the recession plot of the data (Fig. 6c). The quickflow (i.e. fast
646 and baseflow (i.e. slow) recessions are shown, both with slopes of 1.5. The early part of
647 the baseflow (i.e. the bump) is shown by the dashed curve. The sum of the fast recession
648 and the baseflow, which fits the streamflow points, is close to the fast recession at high
649 flow and matches the slow flow recession at low flows, as expected. The slope is steeper
650 at the medium flows between these two end states (the slope is about 6). This emphasises
651 the point that the slope of the streamflow points on a recession plot is meaningless in
652 terms of catchment storages at medium flows. Only the slopes of the quickflow and the
653 late-recession streamflow (which is the same as the late-recession baseflow) have
654 meaning in terms of storage types.

655

656 Fig. 6d shows the fraction of baseflow in the streamflow versus time according to the
657 tracer-based BRM. Baseflow makes up 32% of the streamflow at the highest flow, then
658 rises to 50% in about three hours (0.12 d), 75% at 14 hours (0.6 d) and 95% at 43 hours
659 (1.8 d). The change from early to late recession is shown at 1.8 d.

660

661

662

663 **4 Discussion**

664

665 **4.1 A new baseflow separation method: Advantages and limitations**

666

667 A new baseflow separation method (the BRM method) is presented. Advantages of the
668 method are:

669

670 (1) It simulates the shape of the baseflow or pre-event component determined by tracers
671 more accurately than previous baseflow separation methods. This should mean that it
672 gives more accurate baseflow separations and BFIs, because tracer separation of the
673 hydrograph is regarded as the only objective method. The BRM method involves a rapid
674 response to rainfall (the “bump”) and then a gradual increase with time following rainfall
675 (the “rise”).

676

677 (2) The parameters (f and k) quantifying the baseflow can be determined by fitting the
678 baseflow to tracer hydrograph separations (as illustrated in Section 3.2) or by fitting the
679 sum of the baseflow and a fast recession to the recession hydrograph under the constraint
680 of a BFI determined by flow considerations (as illustrated in Stewart, 2014a).

681

682 (3) The method can be applied using tracer data or streamflow data alone, and

683

684 (4) The method is easy to implement mathematically.

685

686 Current limitations or areas where further research may be needed are:

687

688 (1) Where there is no tracer data, specification of f and k depends on an initial estimate of
689 the BFI, although the optimisation procedure means that this is not critical.

690

691 (2) The method produces an averaged representation of the baseflow hydrograph when
692 applied to long-term data, so seasonal or intra catchment variations are likely.

693

694 (3) Separation of the hydrograph into three or more components (as shown by some
695 tracer studies) could be explored. The next section considers three components.

696

697 **4.2 Calibration of the BRM Algorithm**

698

699 This paper describes and demonstrates two ways of calibrating the BRM method (i.e.
700 determining its parameters f and k). These were also applied to the H & H and Eckhardt
701 methods. These are (1) fitting the methods to tracer separations, and (2) applying an
702 optimizing or other procedure. The tracer-based (first way) is demonstrated in this paper,
703 the optimizing procedure (second way) was demonstrated in the early (unreviewed)
704 version of this paper (Stewart, 2014a) and applied to the Eckhardt method in Stewart
705 (2014b). Additional procedures put forward by Collischon and Fan (2013), based on
706 characteristic flow duration curve flows (Q_{90}/Q_{50}) and a backwards filter, are also
707 compared with the other methods in this paper, but are not considered in detail.

708

709 Tracer separation of streamflow components depends on the tracer or tracers being used
710 and the experimental methods, etc. Klaus and McDonnell (2013) recently reviewed the
711 use of stable isotopes for hydrograph separation and restated the five underlying
712 assumptions. In the present case, deuterium was used by Bonell et al. (1990) to separate
713 the streamflow into event and pre-event components (Fig. 2a). The pre-event component
714 includes all of the water present in the catchment before the recorded rainfall event. The
715 pre-event component therefore includes soil water mobilized during the event as well as
716 groundwater. Three-component tracer separations have often been able to identify soil
717 water contributions along with direct precipitation and groundwater contributions in
718 streamflow (e.g. Iorgulescu et al. (2005) identified direct precipitation, acid soil and
719 groundwater components, Fig. 2b).

720

721 The second way of calibrating the BRM assumes a value for the BFI and then uses this as
722 a constraint to enable the sum (baseflow plus a fast recession) to be fitted to a streamflow
723 recession (winter and summer events were examined in Stewart, 2014a). It is assumed
724 that when the best-fit occurs (i.e. the baseflow has the optimum shape to fit to the
725 streamflow) that the baseflow shape will be most similar to the “true” groundwater shape.
726 The winter event BFI assumed is approximately in agreement with the BFIs given by the
727 H & H and prescribed Eckhardt methods when applied to the 1996 streamflow record
728 (the BFIs given by the H & H, prescribed Eckhardt and winter BRM methods are 0.679,
729 0.617 and 0.622 respectively). If this represents groundwater alone, then the difference
730 with the pre-event water (or the BRM baseflow matched to it) is the soil water component
731 as explained in Stewart (2014a). The groundwater and soil water components derived are

732 shown in Fig. 7 for the 23/2/88 event and two-week period in 1996. The soil water
733 component responds to rainfall more than the groundwater during events, then falls more
734 rapidly after them. In the absence of tracers, it is not generally possible to identify the
735 true groundwater component, but some BFI results appear to be “hydrologically more
736 plausible” than others (quoted phrase from Eckhardt, 2008). The BFI assumed for the
737 groundwater here is considered to be hydrologically plausible.

738

739 **4.3 Why is it necessary to apply baseflow separation to understand the** 740 **hydrograph?**

741

742 The answer is straightforward:

743

744 *Because streamflow is a mixture of quickflow and baseflow components, which have very*
745 *different characteristics and generation mechanisms and therefore give very misleading*
746 *results when analysed as a mixture.*

747

748 Previous authors (e.g. Hall, 1968, Brutsaert and Nieber, 1977, Tallaksen, 1995) addressed
749 “baseflow recession analysis” or “low flow recession analysis” in their titles, but
750 nevertheless included both early and late parts of the recession hydrograph in their
751 analyses. Kirchner (2009, P. 27) described his approach with the statement “the present
752 approach makes no distinction between baseflow and quickflow. Instead it treats
753 catchment drainage from baseflow to peak stormflow and back again, as a single
754 continuum of hydrological behavior. This eliminates the need to separate the hydrograph
755 into different components, and makes the analysis simple, general and portable”. This
756 work contends that catchment runoff is *not* a single continuum, and the varying
757 contributions of two or more very different components need to be kept in mind when the
758 power-law slopes of the points on recession plots are considered. Lack of separation has
759 probably led to misinterpretation of the slopes in terms of catchment storage reservoir
760 types.

761

762 Kirchner’s (2009) approach may be appropriate for his main purpose of “doing hydrology
763 backwards” (i.e. inferring rainfall from catchment runoff), but the current author suggests
764 that it gives misleading information about catchment storage reservoirs (as illustrated by
765 the different slopes of streamflow, quickflow and probably baseflow (Fig. 6c). Likewise
766 Lamb and Beven’s (1997) approach may have been fit-for-purpose for assessing the
767 “catchment saturated zone store”, but by combining parts of the early recession with the
768 late recession may give misleading information concerning catchment reservoir type (and
769 therefore catchment response). Others have used recession analysis on early and late
770 streamflow recessions for diagnostic tests of model structure at different scales (e.g.
771 Clark et al., 2009; McMillan et al., 2011) and it is suggested that these interpretations
772 may have produced misleading information on storage reservoirs.

773

774 Evidence of the very different characteristics and generation mechanisms of quickflow
775 and baseflow are provided by:

776

777 (1) The different timings of their releases to the stream (quick and slow) as shown by the
778 early and late parts of the recession curve. (Note: The rapid response of slow storage
779 water to rainfall (the “bump” in the BRM baseflow hydrograph) does not conflict with
780 this because the bump is due to celerity not to fast storage.)

781

782 (2) Many tracer studies (chemical and stable isotope) have shown differences between
783 quickflow and baseflow, and substantiated their different timings of storage.

784

785 (3) Transit times of streamwaters show great differences between quickflow and
786 baseflow. While quickflow is young (as shown by the variations of conservative tracers
787 and radioactive decay of tritium), baseflow can be much older with substantial fractions
788 of water having mean transit times beyond the reach of conservative tracer variations (4
789 years) and averaging 10 years as shown by tritium measurements (Stewart et al., 2010).

790

791 These considerations show that quickflow and baseflow are very different and in
792 particular have very different hydrographs, so their combined hydrograph (streamflow)
793 does not reflect catchment characteristics (except at low flows when there is no
794 quickflow).

795

796 **4.4 A new approach to recession analysis**

797

798 It appears that streamflow recession analysis is a technique in disarray (Stoelzle et al.,
799 2013). Different methods give different results and there is “a continued lack of
800 consensus on how to interpret the cloud of data points” (Brutsaert, 2005). This work
801 asserts that recession studies have been giving misleading results in regard to catchment
802 functioning because streamflow is a varying mixture of components (unless the studies
803 were applied to late recessions only). The new approach of applying recession analysis to
804 the separated quickflow component as well as streamflow may help to resolve this
805 confusion, by demonstrating the underlying structure due to the different components in
806 recession plots (as illustrated in Fig. 6c). Plotting baseflow from the late part of the
807 recession may also be helpful. In particular, it is believed that recession analysis on
808 quickflow, and late recession baseflow as well as streamflow will give information that
809 actually pertains to those components, giving a clearer idea than ever before on the nature
810 of the water storages in the catchment, and contributing to broader goals such as
811 catchment characterisation, classification and regionalisation.

812

813 Observations from the limited data set in this paper and from some other catchments to be
814 reported elsewhere are:

815

816 (1) Quickflow appears to be quadratic in character (Section 7.2). This may result from a
817 variety of processes such as surface detention, passage through saturated zones within the
818 soil (perched zones) or within riparian zones near the stream. Whether this is true of
819 catchments in a wider variety of climatic regimes remains to be seen.

820

821 (2) The baseflow reservoirs at Glendhu appear to be quadratic in character, as has been
822 previously observed at many other catchments by other authors (Brutsaert and Nieber,
823 1977; Wittenberg, 1999; Dewandel, 2005; Stoelzle et al., 2013). Hillslope and valley
824 groundwater aquifers feed the water slowly to the stream.

825

826 (3) The many cases of high power-law slopes ($d > 1.5$) in recession plots reported in the
827 literature appear to be artifacts due to plotting early recession streamflow (particularly in
828 the mid-flow range) instead of separated components. This may have also contributed to
829 the wide scatter of points generally observed in recession plots (referred to as “high time
830 variability in the recession curve” by Tallaksen, 1995).

831

832 (4) The most problematic parts of streamflow recession curves are those at intermediate
833 flows when quickflow and baseflow are approximately equal. This is where steep power-
834 law slopes are found. Data at high flows are dominated by quickflow, and baseflow
835 contributes almost all of the flow at low flows, so these parts do not have high power-law
836 slopes.

837
838 (5) Some other causes of scatter in recession plots are: insufficient accuracy of
839 measurements at low flows (Rupp and Selker, 2002), effects of rainfall during recession
840 periods (most data selection methods try to exclude these), different rates of
841 evapotranspiration in different seasons, different effects of rainfall falling in different
842 parts of the catchment, and drainage from different aquifers in different dryness
843 conditions. These effects will be able to be examined more carefully when the
844 confounding effects of baseflow are removed from intermediate flows.

845
846 (6) Splitting the recession curve into early and late portions based on baseflow separation
847 turns out to be a very useful thing to do. The early part has quickflow plus the
848 confounding effects of baseflow, while the late part has only baseflow. The late part starts
849 when baseflow becomes predominant (>95%, Fig. 6d), this can be calculated by
850 identifying the point where $B_t/Q_t = 0.95$ during a recession. The separation can be made
851 It appears that at Glendhu, the inflexion point records a change of slope *in the baseflow*
852 and lies within the early part of the recession.

853
854 (7) The close links between surface water hydrology and groundwater hydrology are
855 revealed as being even closer by this work. Baseflow is mostly groundwater, and
856 quickflow is also starting to look distinctly groundwater-influenced (or saturation-
857 influenced). The success of groundwater models (Gusyev et al., 2013, 2014) in
858 simulating tritium concentrations and baseflows in streams while being calibrated to
859 groundwater levels in wells shows the intimate connection between the two. The feeling
860 that catchment drainage can be treated as a single continuum of hydrological behavior has
861 probably prevented recognition of the disparate natures of the quick and slow drainages.
862 This may be a symptom of the fact that surface water hydrology and groundwater
863 hydrology can be regarded as different disciplines (Barthel, 2014). Others however are
864 crossing the divide by examining geological controls on BFIs (Bloomfield et al., 2009)
865 and relating baseflow simulation to aquifer model structure (Stoelzle et al., 2014).

866
867
868
869

870 **5 Conclusions**

871
872 This paper has two main messages. The first is the introduction of a new baseflow
873 separation method (the bump and rise method or BRM). The advantage of the BRM is
874 that it enables simulation of the shape of the baseflow or pre-event component
875 determined by tracers more accurately than previous methods. Tracer separations are
876 regarded as the only objective way of determining baseflow separations and BFIs, so the
877 BRM method should give more accurate baseflow separations and BFIs. The BRM
878 parameters are determined by either fitting them to tracer separations (which are usually
879 determined on a small number of events) as illustrated in this paper, or by estimating the
880 BFI and using it as a constraint which enables determination of the BRM parameters by
881 an optimization procedure on an event or events as illustrated in an earlier version of this

882 paper (Stewart, 2014a). The BRM algorithm can then be simply applied to the entire
883 streamflow record.

884

885 Current limitations or areas where further research could be needed are: (1) specification
886 of f and k depends on tracer information or an initial estimate of the BFI, although the
887 optimisation procedure means that this is not critical, (2) the method applied to long-term
888 data produces an averaged representation of the baseflow hydrograph, so seasonal or intra
889 catchment variations are likely, and (3) separation of the hydrograph into three
890 components (as shown by some tracer studies) could be explored (and has been for the
891 Glendhu Catchment).

892

893 The second main message is that recession analysis of streamflow alone on recession
894 plots can give very misleading results regarding the nature of catchment storages because
895 streamflow is a varying mixture of components. Instead, plotting separated quickflow
896 gives insight into the early recession flow sources (high to mid flows), and separated
897 baseflow (which is equal to streamflow) gives insight into the late recession flow sources
898 (low flows). The very different behaviours of quickflow and baseflow are evident from
899 their different timings of release from storage (shown by the early and late portions of the
900 recession curve, by tracer studies, and by their very different transit times). Clearer ideas
901 on the nature of the storages in the catchment can contribute to broader goals such as
902 catchment characterisation, classification and regionalization, as well as modelling. Flow
903 duration curves can also be determined for the separated stream components, and these
904 help to illuminate the makeup of the streamflow at different exceedance percentages.

905

906 Conclusions drawn from applying recession analysis to separated components in this
907 paper are: (1) Many cases of high power-law slopes ($d > 1.5$) in recession plots reported in
908 the literature are likely to be artifacts due to plotting early recession streamflow instead of
909 quickflow. The most problematic parts of streamflow recession curves are those at
910 intermediate flows when quickflow and baseflow are approximately equal. This is where
911 steep power-law slopes are found. (2) Both quickflow and baseflow reservoirs appear to
912 be quadratic in character, suggesting that much streamwater passes through saturated
913 zones (perched zones in the soil, riparian zones, groundwater aquifers) at some stage. (3)
914 Other causes of scatter in recession plots will be able to be examined more carefully
915 when the confounding effects of baseflow are removed from intermediate flows. (4)
916 Splitting the recession curve into early and late portions is very informative, because of
917 their different makeups. The late part starts when baseflow becomes predominant.

918

919 Some suggestions for the way forward in light of the findings of this paper are: (1)
920 Recession analyses (and transit time analyses and chemical/discharge relationships)
921 should be qualified with the component being analysed. This will make the significance
922 of the results clearer. (2) Rainfall-runoff models should make more use of (non-linear)
923 quadratic storage systems for simulating streamflow. (3) Much more data on many other
924 catchment areas needs to be examined in this way to develop and refine these concepts.

925

926

927 **6 Acknowledgements**

928

929 I thank Barry Fahey, John Payne and staff of Landcare Research NZL for data and
930 cooperation on Glendhu Catchment studies.

931

932 **7 References**

- 933
- 934 Bazemore, D. E., Eshleman, K. N. and Hollenbeck, K. J.: The role of soil water in
935 stormflow generation in a forested headwater catchment: synthesis of natural
936 tracer and hydrometric evidence, *J. Hydrol.*, 162, 47-75, 1994.
- 937 Barthel, R.: HESS Opinions “Integration of groundwater and surface water research: an
938 interdisciplinary problem?”, *Hydrol. Earth Syst. Sci.*, 18, 2615-2628, 2014.
- 939 Beven, K. J.: Hydrograph separation? In Proceedings of the BHS 3rd National Hydrology
940 Symposium, Southampton, 1991.
- 941 Beven, K. J.: Rainfall-runoff modelling: the primer, 2nd ed. Wiley-Blackwell, Chichester.
942 2012.
- 943 Biswal, B. and Marani M.: Geomorphological origin of recession curves. *Geophys. Res.*
944 *Lett.*, 37: L24403, 2010.
- 945 Bloomfield, J. P., Allen, D. J. and Griffiths K. J.: Examining geological controls on
946 baseflow index (BFI) using regression analysis: An illustration from the Thames
947 Basin, UK, *J. Hydrol.*, 373 (1–2), 164-176, 2009.
948 doi:10.1016/j.jhydrol.2009.04.025
- 949 Bonell, M., Pearce, A. J. and Stewart M. K.: Identification of runoff production
950 mechanisms using environmental isotopes in a tussock grassland catchment,
951 Eastern Otago, New Zealand, *Hydrol. Processes*, 4(1), 15-34, 1990.
- 952 Boussinesq, J.: Essai sur la théorie des eaux courantes, *Memoires de l’Académie des*
953 *Sciences de l’Institut de France*, 23, 252–260, 1877.
- 954 Boussinesq, J.: Sur un mode simple d’e coulement des nappes d’eau d’infiltration a` lit
955 horizontal, avec rebord vertical tout autour lorsqu’une partie de ce rebord est
956 enlevée depuis la surface jusqu’au fond, *C. R. Acad. Sci.*, 137, 5–11, 1903.
- 957 Bowden, W. B., Fahey, B. D., Ekanayake, J. and Murray, D. L.: Hillslope and wetland
958 hydrodynamics in a tussock grassland, Southland, New Zealand, *Hydrol.*
959 *Processes*, 15, 1707–1730, 2001.
- 960 Brutsaert, W. and Nieber J. L.: Regionalized drought flow hydrographs from a mature
961 glaciated plateau, *Water Resour. Res.*, 13(3), 637-643, 1977.
- 962 Brutsaert, W.: *Hydrology: An Introduction*, Cambridge University Press, Cambridge,
963 UK, 605 pp., 2005.
- 964 Buttle, J. M.: Isotope hydrograph separations and rapid delivery of pre-event water from
965 drainage basins, *Prog. Phys. Geog.*, 18, 16-41, 1994.
- 966 Campbell, D. I., and Murray, D. L.: Water balance of snow tussock grassland in New
967 Zealand. *J. Hydrol.*, 118, 229-245, 1990.
- 968 Chapman, T. G.: A comparison of algorithms for streamflow recession and baseflow
969 separation, *Hydrol. Processes*, 13, 701-714, 1999.
- 970 Chapman, T. G. and Maxwell A. I.: Baseflow separation - Comparison of numerical
971 methods with tracer experiments, In Proceedings of the 23rd Hydrology and Water
972 Resources Symposium. Hobart, Australia, 539-545, 1996.
- 973 Clark, M. P., Rupp, D. E., Woods, R. A., Tromp-van Meerveld, H. J., Peters, N. E. and
974 Freer J. E.: Consistency between hydrological models and field observations:
975 linking processes at the hillslope scale to hydrological responses at the watershed
976 scale, *Hydrol. Process.*, 33, 311-319, 2009.
- 977 Collischon, W. and Fan, F. M.: Defining parameters for Eckhardt’s digital baseflow filter.
978 *Hydrol. Process.* 27, 2614-2622. DOI: 10.1002/hyp.9391, 2013.
- 979 Dewandel, B., Lachassagne, P., Bakalowicz, M., Weng, P. and Al-Malki, A.: Evaluation
980 of aquifer thickness by analysing recession hydrographs. Application to the Oman
981 ophiolite hard-rock aquifer, *J. Hydrol.*, 274, 248-269, 2003.

982 Eckhardt, K.: How to construct recursive digital filters for baseflow separation, *Hydrol.*
983 *Process.*, 19, 507–515. DOI: 10.1002/hyp.5675, 2005.

984 Eckhardt, K.: A comparison of baseflow indices, which were calculated with seven
985 different baseflow separation methods, *J. Hydrol.*, 352, 168-173, 2008.

986 Fahey, B. D., and Jackson, R. J.: Hydrological impacts of converting native forest and
987 grasslands to pine plantations, South Island, New Zealand, *Agric. Forest*
988 *Meteorol.*, 84, 69–82, 1997.

989 Fenicia, F., Kavetski, D. and Savenije H. H. G.: Elements of a flexible approach for
990 conceptual hydrological modelling: 1. Motivation and theoretical development,
991 *Water Resour. Res.*, 47, W11510, doi:10.1029/2010WR010174, 2011.

992 Fenicia, F., Savenije, H. H. G., Matgen, P. and Pfister, L.: Is the groundwater reservoir
993 linear? Learning from data in hydrological modeling, *Hydrol. Earth Syst. Sci.*,
994 10(1), 139-150, 2006.

995 Gonzales, A. L., Nonner, J., Heijers, J. and Uhlenbrook, S.: Comparison of different
996 baseflow separation methods in a lowland catchment, *Hydrol. Earth Syst. Sci.*, 13,
997 2055-2068, 2009.

998 Gusyev, M. A., Abrams, D., Toews, M. W., Morgenstern, U., Stewart, M. K.: A
999 comparison of particle-tracking and solute transport methods for
1000 simulation of tritium concentrations and groundwater transit times in river
1001 water. *Hydrol. Earth Syst. Sci.*, 18, 3109-3119. 2014. doi:10.5194/hess-18-
1002 3109-2014

1003 Gusyev, M.A., Toews, M. W., Morgenstern, U., Stewart, M. K. and Hadfield, J.:
1004 Calibration of a transient transport model to tritium measurements in rivers and
1005 streams in the western Lake Taupo catchment, New Zealand, *Hydrol. Earth Syst.*
1006 *Sci.*, 17, 1217-1227, 2013.

1007 Hall, F. R.: Base-flow recessions – A review, *Water Resour. Res.*, 4, 975-983, 1968.

1008 Hangen, E., Lindenlaub, M., Leibundgut, Ch. and von Wilpert, K.: Investigating
1009 mechanisms of stormflow generation by natural tracers and hydrometric data: a
1010 small catchment study in the Black Forest, Germany, *Hydrol. Processes*, 15, 183-
1011 199, 2001.

1012 Hewlett, J.D. and Hibbert, A. R.: Factors affecting the response of small watersheds to
1013 precipitation in humid areas, in *Forest Hydrology*, edited by W. E. Sopper and H.
1014 W. Lull, pp. 275–290, Pergamon, Oxford, 1967.

1015 Hrachowitz, M., Savenije, H., Bogaard, H., Tetzlaff, D. and Soulsby C.: What can flux
1016 tracking teach us about water age distributions and their temporal dynamics?
1017 *Hydrol. Earth Syst. Sci.*, 17, 533-564, 2013.

1018 Holko, L., Herrmann, A., Uhlenbrook, S., Pfister, L. and Querner E.: Ground water
1019 runoff separation – test of applicability of a simple separation method under
1020 varying natural conditions, *Friend 2002 – Regional hydrology: Bridging the gap*
1021 *between research and practice (IAHS Publication no. 274)*, 265-272, 2002.

1022 Hooper, R.P. and Shoemaker, C. A.: A comparison of chemical and isotopic hydrograph
1023 separation, *Water Resour. Res.*, 22, 1444-1454, 1986.

1024 Iorgulescu, I., Beven, K. J. and Musy, A.: Data-based modelling of runoff and chemical
1025 tracer concentrations in the Haute-Mentue research catchment (Switzerland),
1026 *Hydrol. Processes*, 19, 2557-2573, 2005.

1027 Iwagami, S., Tsujimura, M., Onda, Y., Shimada, J. and Tanaka T.: Role of bedrock
1028 groundwater in the rainfall–runoff process in a small headwater catchment
1029 underlain by volcanic rock, *Hydrol. Processes*, 24, 2771-2783. DOI:
1030 10.1002/hyp.7690, 2010.

1031 Joerin, C., Beven, K. J., Iorgulescu, I. and Musy A.: Uncertainty in hydrograph
1032 separations based on mixing models. *J. Hydrol.*, 255, 90-106, 2002.

1033 Kirchner, J. W.: Catchments as simple dynamical systems: Catchment characterization,
1034 rainfall-runoff modelling, and doing hydrology backward, *Water Resour. Res.*,
1035 45:W02429, doi:10.1029/2008WR006912, 2009.

1036 Klaus, J. and McDonnell, J. J.: Hydrograph separation using stable isotopes: Review and
1037 evaluation, *J. Hydrol.*, 505, 47-64, 2013.

1038 Lamb, R. and Beven, K. J.: Using interactive recession curve analysis to specify a general
1039 catchment storage model, *Hydrol. Earth Syst. Sci.*, 1, 101-103, 1997.

1040 Linsley, R. K., Kohler, M. A. and Paulhus, J. L.: *Hydrology for Engineers*, McGraw-Hill,
1041 New York, 1975.

1042 Lyne, V. D., Hollick, M. Stochastic time-variable rainfall runoff modelling. *Hydrology
1043 and Water Resources Symposium*, Institution of Engineers Australia, Perth. 89-
1044 92, 1979.

1045 McDonnell, J. J., Beven, K. J.: Debates – The future of Hydrological Sciences: A
1046 (common) path forward? A call to action aimed at understanding velocities,
1047 clerities and residence time distributions of the headwater hydrograph, *Water
1048 Resour. Res.*, 80, 5342-5350, 2014. Doi:10.1002/2013WR015141.

1049 McDonnell, J. J., Bonell, M., Stewart, M. K. and Pearce, A. J.: Deuterium variations in
1050 storm rainfall – Implications for stream hydrograph separation, *Water Resour.
1051 Res.*, 26, 455-458, 1991.

1052 McMillan, H. K., Clark, M. P., Bowden, W. B., Duncan, M. and Woods, R.:
1053 Hydrological field data from a modeller’s perspective: Part 1. Diagnostic tests for
1054 model structure, *Hydrol. Process.* 25, 511-522, 2011.

1055 Michel, R. L., Aggarwal, P., Araguas-Araguas, L., Kurttas, T., Newman, B. D. and
1056 Vitvar, T.: A simplified approach to analyzing historical and recent tritium data in
1057 surface waters, *Hydrol. Processes*, DOI: 10.1002/hyp. 10174, 2014.

1058 Nejadhashemi, A. P., Shirmohammadi, A. and Montas, H. J.: Evaluation of streamflow
1059 partitioning methods, Pap. No. 032183 in ASAE Annual International Meeting,
1060 edited by M. St. Joseph M, Las Vegas, Nevada, USA, 2003.

1061 Pearce, A. J., Rowe, L. K. and O’Loughlin, C. L.: Hydrology of mid-altitude tussock
1062 grasslands, upper Waipori catchment, Otago: II Water balance, flow duration and
1063 storm runoff, *J. Hydrol. (NZ)*, 23, 60-72, 1984.

1064 Pfister, L., McDonnell, J. J., Hissler, Ch., Klaus, J., Stewart M. K.: Geological controls
1065 on catchment mixing, storage, and release. *Hydrol. Process.*, in review, 2014.

1066 Pinder, G. F. and Jones, J. F.: Determination of the ground-water component of peak
1067 discharge from the chemistry of total runoff. *Water Resour. Res.*, 5, 438–445.
1068 DOI:10.1029/WR005i002p00438, 1969.

1069 Rupp, D. E. and Selker, J. S.: Information, artifacts and noise in $dQ/dt - Q$ recession
1070 analysis, *Adv. Water Resour.*, 29, 154-160, 2006.

1071 Searcy, R. K.: Flow-duration curves, *Manual of Hydrology: Part 2. Low-flow techniques*,
1072 Geological Survey Water-Supply paper 1542-A, 33 p, 1959.

1073 Shaw, S. B. and Riha, J. S.: Examining individual recession events instead of a data
1074 cloud: Using a modified interpretation of $dQ/dt-Q$ streamflow recession in
1075 glaciated watersheds to better inform models of low flow, *J. Hydrol.*, 434-435, 46-
1076 54, 2012.

1077 Sklash, M. G. and Farvolden, R. N.: The role of groundwater in storm runoff, *J. Hydrol.*,
1078 43, 45-65, 1979.

1079 Sloto, R. A. and Crouse, M. Y.: HYSEP: A computer program for streamflow hydrograph
1080 separation and analysis, US Geological Survey, Water-Resources Investigations
1081 Report 96-4040, 1996.

1082 Smakhtin, V. U.: Low flow hydrology: A review, *J. Hydrol.*, 240, 147-186, 2001.

1083 Stewart, M. K.: New baseflow separation and recession analysis approaches for
1084 streamflow. *Hydrol. Earth Syst. Sci., Discuss.*, 11, 7089-7131, 2014a.
1085 doi:10.5194/hessd-11-7089-2014

1086 Stewart, M. K.: Interactive comment on “New baseflow separation and recession analysis
1087 approaches for streamflow” by M. K. Stewart, *Hydrol. Earth Syst. Sci. Discuss.*,
1088 11, C3964-C3964, 2014b.

1089 Stewart, M. K. and Fahey, B. D.: Runoff generating processes in adjacent tussock
1090 grassland and pine plantation catchments as indicated by mean transit time
1091 estimation using tritium, *Hydrol. Earth Syst. Sci.*, 14, 1021-1032, 2010.

1092 Stewart, M.K., Mehlhorn, J. and Elliott, S.: Hydrometric and natural tracer (^{18}O , silica, ^3H
1093 and SF_6) evidence for a dominant groundwater contribution to Pukemanga
1094 Stream, New Zealand, *Hydrol. Processes*, 21(24), 3340-3356.
1095 DOI:10.1002/hyp.6557, 2007.

1096 Stewart, M. K., Morgenstern, U. and McDonnell, J. J.: Truncation of stream residence
1097 time: How the use of stable isotopes has skewed our concept of streamwater age
1098 and origin, *Hydrol. Processes*, 24(12), 1646-1659, 2010.

1099 Stewart, M. K., Morgenstern, U., McDonnell, J. J. and Pfister, L.: The “hidden
1100 streamflow” challenge in catchment hydrology: A call to action for
1101 streamwater transit time analysis, *Hydrol. Processes* 26(13), 2061-2066.
1102 doi: 10.1002/hyp.9262, 2012.

1103 Stoelzle, M., Stahl, K. and Weiler, M.: Are streamflow recession characteristics really
1104 characteristic? *Hydrol. Earth Syst. Sci.*, 17, 817-828, 2013.
1105
1106

1107 Stoelzle, M., Weiler, M., Stahl, K., Morhard, A. and Schuetz, T.: Is there a superior
1108 conceptual groundwater model structure for baseflow simulation?, *Hydrol.*
1109 *Process.* 2014. DOI: 10.1002/hyp.10251

1110 Su, N. G.: The Unit-Hydrograph Model for Hydrograph Separation, *Environ. Internat.*,
1111 21, 509-515, 1995.

1112 Tallaksen, L.M.: A review of baseflow recession analysis, *J. Hydrol.*, 165, 349-370,
1113 1995.

1114 Vogel, R. and Kroll, C.: Regional geohydrogeologic-geomorphic relationships for the
1115 estimation of low-flow statistics, *Water Resour. Res.*, 28, 2451-2458, 1992.

1116 Westerberg, I. K., Guerrero, J.-L., Younger, P. M., Beven, K. J., Seibert, J., Halldin, S.,
1117 Freer, J. E. and Xu, C.-Y.: Calibration of hydrological models using flow-duration
1118 curves, *Hydrol. Earth Syst. Sci.*, 15, 2205-2227, 2011.

1119 Wittenberg, H.: Baseflow recession and recharge as nonlinear storage processes, *Hydrol.*
1120 *Processes*, 13, 715-726, 1999.

1121 Zhang, R., Li, Q., Chow, T. L., Li, S. and Danielescu, S.: Baseflow separation in a small
1122 watershed in New Brunswick, Canada, using a recursive digital filter calibrated
1123 with the conductivity mass balance method, *Hydrol. Processes*, 27, 2659-2665,
1124 2013.
1125
1126

1127 Table 1. Tracer calibration of the baseflow separation methods by comparison with pre-
 1128 event water determined using deuterium for a streamflow event on 23 February 1988 at
 1129 Glendhu GH1 Catchment (Bonell et al., 1990). The listed parameters were determined as
 1130 described in the text. The standard deviations (sd) show the goodness of fit between the
 1131 various baseflows and the pre-event water.

Separation Method	BFI ^a	f ^a	k ^a mmd ⁻¹ h ⁻¹	BFI _{max} ^a	a ^a h ⁻¹	sd mmd ⁻¹
Pre-event water	0.529	--	--	--	--	--
H & H	0.255	--	0.0472	--	--	6.41
Eckhardt (prescribed)	0.272	--	--	0.8	0.9982	6.34
Eckhardt (optimised)	0.524	--	--	0.886	0.991	5.40
BRM	0.526	0.4	0.009	--	--	1.98

1132 ^aBFI is baseflow index, f bump fraction, k slope parameter, BFI_{max} maximum value of the
 1133 baseflow index that can be modelled by the Eckhardt algorithm, and a recession constant.
 1134
 1135
 1136
 1137
 1138

1139 Table 2. BFIs and parameters of the baseflow separation methods applied to the hourly
 1140 streamflow record in 1996, and to the master recession curve. The Q_{90}/Q_{50} ratio is from
 1141 the flow duration curve for 1996, and the FDC BFI_{max} and FDC BFI are from equations
 1142 20 and 21 in the text.

Separation Method	BFI ^a	f ^a	k ^a mmd ⁻¹ h ⁻¹	BFI _{max} ^a	a ^a h ⁻¹
Q_{90}/Q_{50}	0.728	--	--	--	--
FDC BFI_{max} (eqn 20)	--	--	--	0.824	--
FDC BFI (eqn 21)	0.779	--	--	--	--
H & H	0.679	--	0.0472	--	--
Eckhardt (prescribed)	0.617	--	--	0.8	0.9982
Eckhardt (back filter)	0.521	--	--	0.593	0.9982
Eckhardt (optimised)	0.754	--	--	0.886	0.991
Eckhardt (back filter)	0.580	--	--	0.668	0.991
BRM	0.780	0.4	0.009	--	--
Master recession curve	0.828	0.4	0.009	--	--

1143 ^aBFI is baseflow index, f bump fraction, k slope parameter, BFI_{max} maximum value of the
 1144 baseflow index that can be modelled by the Eckhardt algorithm, and a recession constant.
 1145

1146 **Figure Captions**

1147

1148 Figure 1 Quickflow and baseflow components of streamflow, and the early and late parts
1149 of the recession curve. Quickflow is represented by the area between the streamflow and
1150 baseflow curves, and baseflow is the area under the baseflow curve.

1151

1152 Figure 2 Tracer hydrograph separation results. (a) Event/pre-event water separation from
1153 catchment GH1, Glendhu, New Zealand using deuterium (replotted from Bonell et al.,
1154 1990). (b) Three component separation from Haute-Mentue research catchment,
1155 Switzerland using silica and calcium (replotted from Iorgulescu et al., 2005). R/F is
1156 rainfall, SF streamflow and the flow components are DP direct precipitation, AS acid soil
1157 and GW groundwater.

1158

1159 Figure 3 Map of Glendhu catchments (GH1 and GH2). The inset shows their location in
1160 the South Island of New Zealand.

1161

1162 Figure 4 (a, c, e) Application of the three baseflow separation methods to fit the pre-event
1163 component determined by deuterium measurements at Glendhu GH1 Catchment for an
1164 event on 23/2/88. The parameters determined by fitting are given in Table 2. (b, d, f)
1165 Baseflows resulting from the best-fit parameters for a two-week period in 1996. Note the
1166 logarithmic scales.

1167

1168 Figure 5. (a-c) Recession plots showing streamflow, baseflow and quickflow from the
1169 1996 GH1 hourly flow record. The line through the mid-flow streamflow and baseflow
1170 points has slope of 6.0, and that through the higher flow quickflow points (flows greater
1171 than 1 mm/d) has slope of 1.5. (d) Flow duration curve showing streamflow, baseflow
1172 and quickflow.

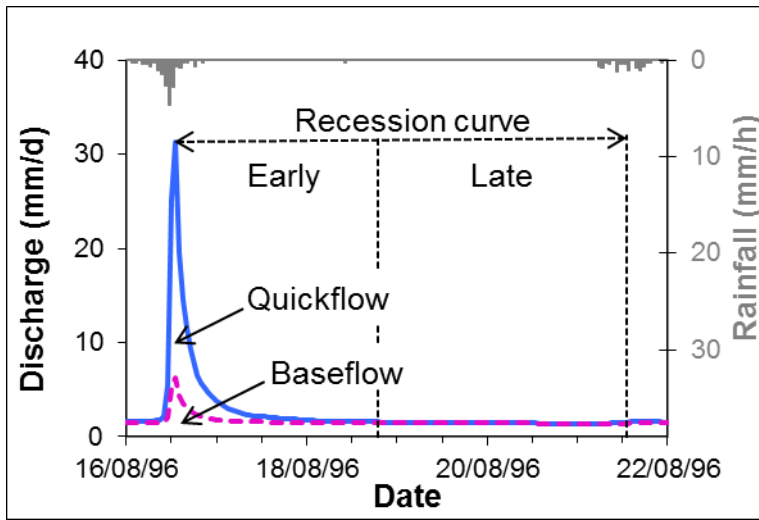
1173

1174 Figure 6. (a) "Master" recession curve for Glendhu GH1 catchment (redrawn from Pearce
1175 et al., 1984). (b) Master recession data matched by the sum of the baseflow and a fast
1176 recession curve. The arrow shows the inflexion point. Early and late parts of the master
1177 recession curve are shown. (c) Recession plot of master recession curve (sum), baseflow
1178 and fast recession. The sum is close to the fast recession curve at high flows and close to
1179 the baseflow (slow recession curve) at low flows. The dashed part of the curve shows the
1180 "bump" in the baseflow. (d) Variation of the baseflow contribution to streamflow with
1181 time during the master recession curve.

1182

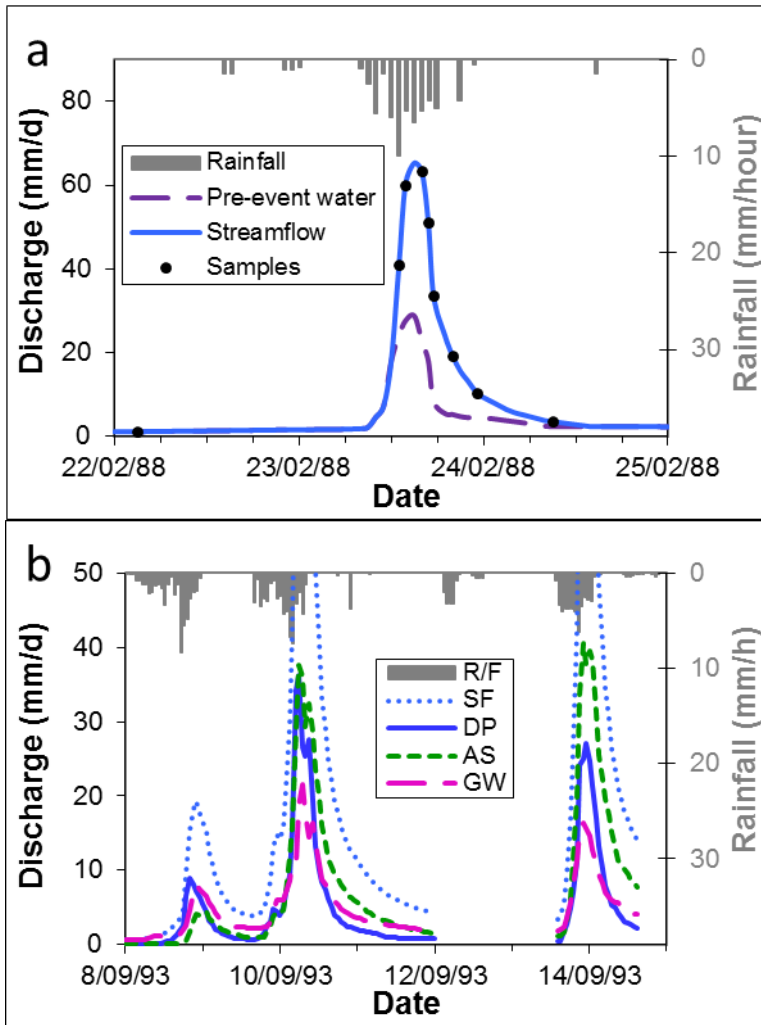
1183 Figure 7 (a, b) Plots showing groundwater and soil water components of the baseflow
1184 matched to the pre-event hydrograph. Streamflow is pre-event water plus event water.

1185



1186

1187 Figure 1 Quickflow and baseflow components of streamflow, and the early and late parts
 1188 of the recession curve. Quickflow is represented by the area between the streamflow and
 1189 baseflow curves, and baseflow is the area under the baseflow curve.
 1190



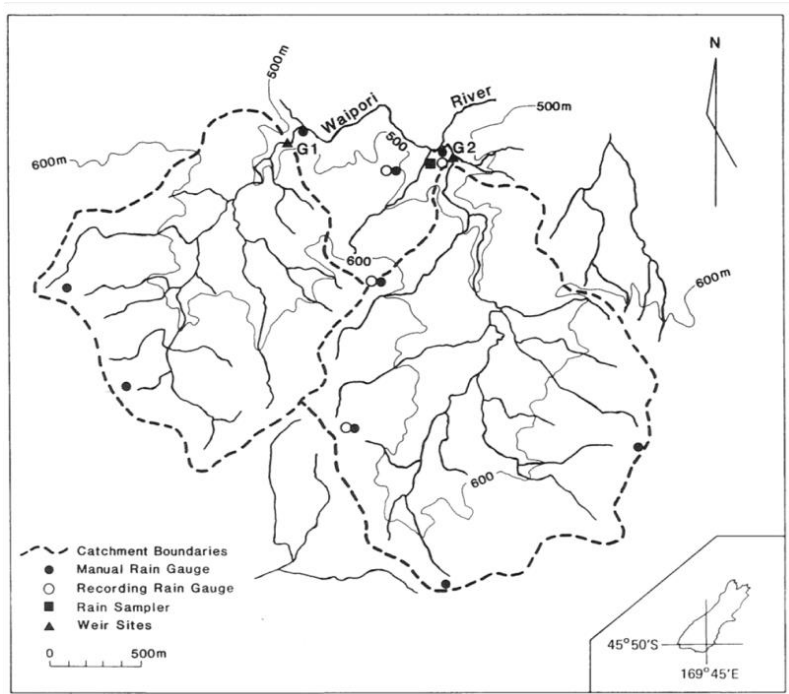
1191

1192

1193

1194 Figure 2 Tracer hydrograph separation results. (a) Event/pre-event water separation from
 1195 catchment GH1, Glendhu, New Zealand using deuterium (replotted from Bonell et al.,
 1196 1990). (b) Three component separation from Haute-Mentue research catchment,
 1197 Switzerland, using silica and calcium (replotted from Iorgulescu et al., 2005). R/F is
 1198 rainfall, SF streamflow and the flow components are DP direct precipitation, AS acid soil
 1199 and GW groundwater

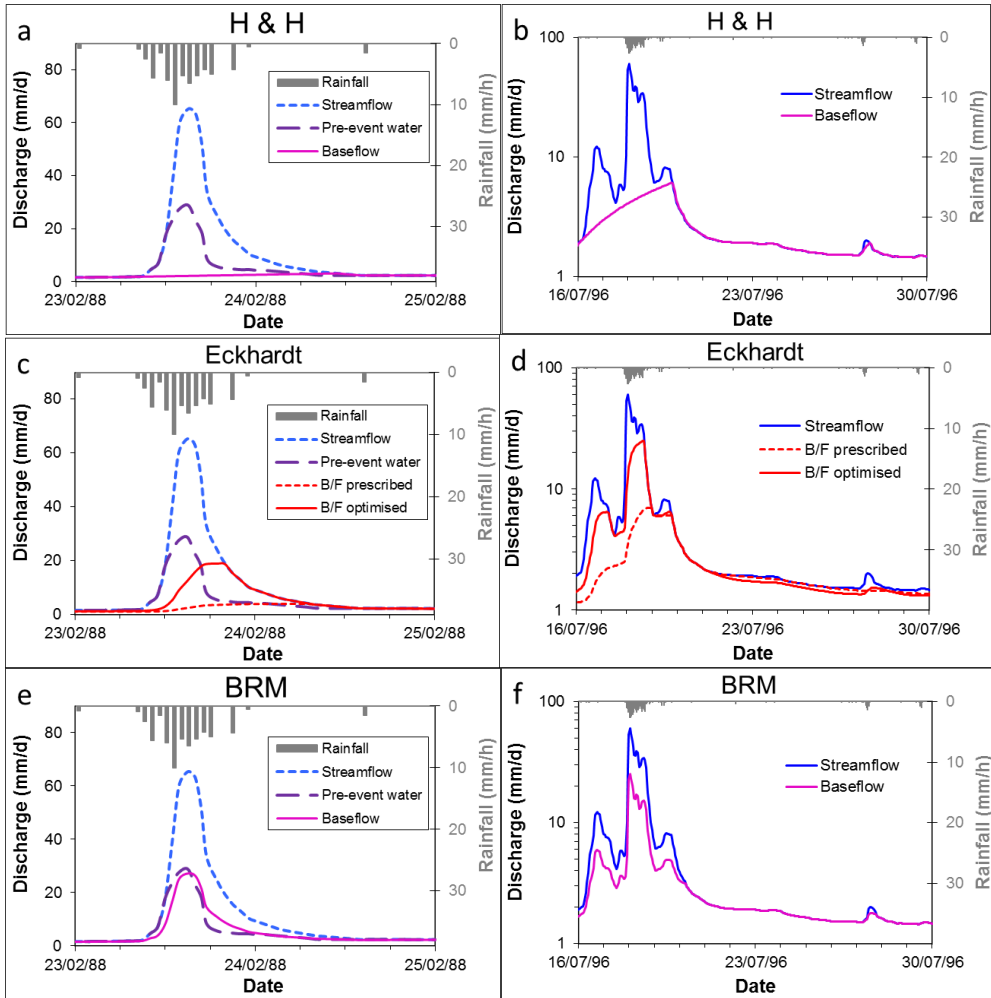
1200



1201

1202 Figure 3 Map of Glendhu catchments (GH1 and GH2). The inset shows their location in
 1203 the South Island of New Zealand.
 1204

1205



1206

1207

1208

1209

1210

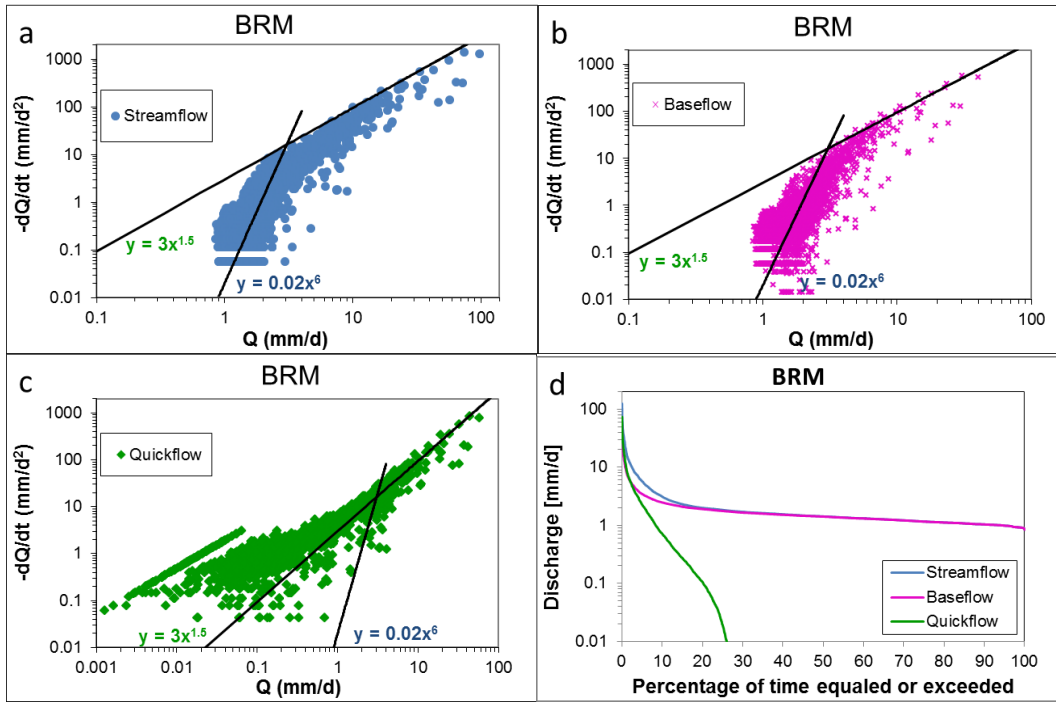
1211

1212

1213

Figure 4 (a, c, e) Fits of the three baseflow separation methods to pre-event water determined by deuterium measurements at Glendhu GH1 Catchment for an event on 23/2/88. The parameters determined by fitting are given in Table 1. (b, d, f) Baseflows resulting from the best-fit parameters for a two-week period in 1996. Note the logarithmic vertical scales.

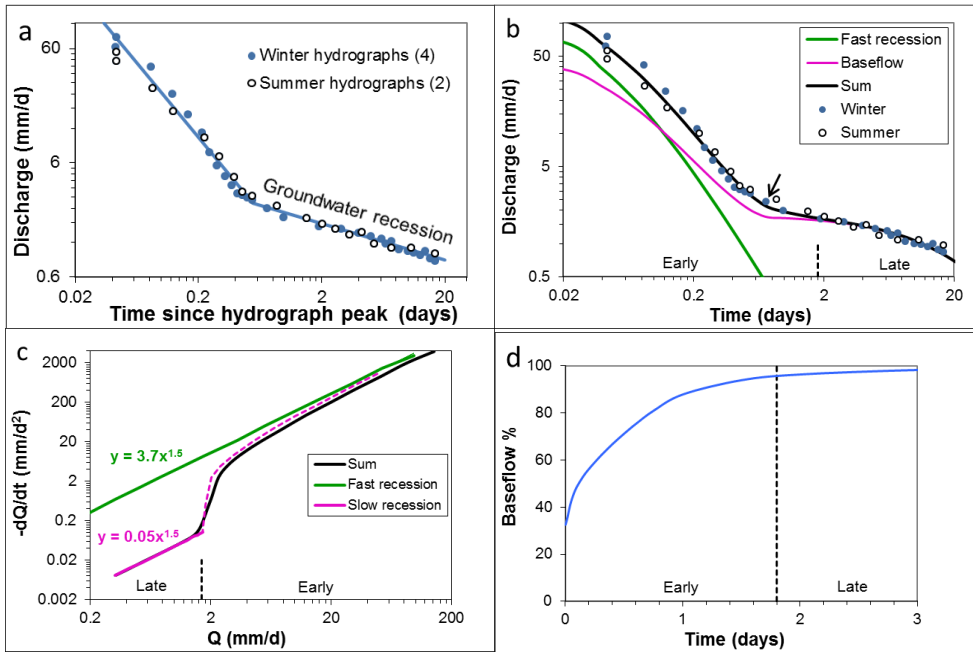
1214



1215
1216
1217
1218
1219
1220
1221
1222

Figure 5 (a-c) Recession plots showing streamflow, baseflow and quickflow from the 1996 GH1 flow record using the BRM method. The line through the mid-flow streamflow and baseflow points has slope of 6.0, and that through the higher flow quickflow points (flows greater than 1 mm/d) has slope of 1.5. Note the wider range of the horizontal axis in (c). (d) Flow duration curve showing streamflow, baseflow and quickflow.

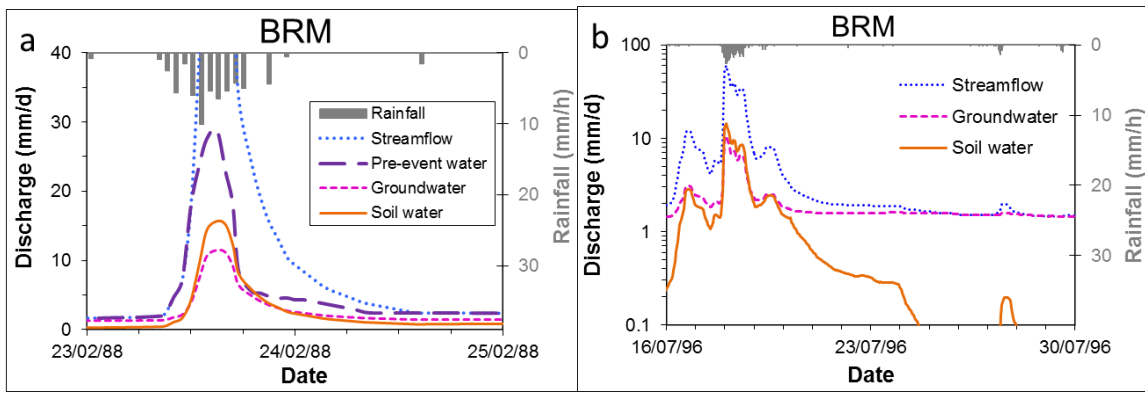
1223



1224
1225
1226
1227
1228
1229
1230
1231
1232
1233

Figure 6 (a) “Master” recession curve for Glendhu GH1 catchment (redrawn from Pearce et al., 1984). (b) Master recession data matched by the sum of the BRM baseflow and fast recession curve. The arrow shows the inflexion point. Early and late parts of the master recession curve are shown. (c) Recession plot of master recession curve (sum), baseflow and fast recession. The sum is close to the fast recession curve at high flows and close to the baseflow (slow recession curve) at low flows. The dashed curve shows the “bump” in the baseflow. (d) Variation of the baseflow contribution to streamflow with time during the master recession curve.

1234



1235

1236

1237

1238

Figure 7 (a, b) Plots showing groundwater and soil water components of the baseflow matched to the pre-event hydrograph. Streamflow is pre-event water plus event water.